Carbonates and Evaporites (2019) 34:525–544
https://doi.org/10.1007/s13146-019-00503-5

REVIEW

Depositional facies and stratal cyclicity of carbonate successions in the Yingshan and Yijianfang Group (Lower-Middle Ordovician) in Yuejin-Tuoputai Region, Tarim Basin, NW China

Cunli Jiao[1] · Zhao Xue-Qin[2] · Rui Zhao[1] · Li Hui-Li[1] · Liu Tian-Jia[2] · Zhao Jia-Hui[2]

Accepted: 4 April 2019 / Published online: 19 April 2019

Abstract

The Lower-Middle Ordovician Yingshan and Yijianfang Group in the Tarim Basin are overwhelmingly composed of cyclic carbonates. Based on microscopic observation and facies analysis from two borehole sections in Yuejin-Tuoputai area, two main types of facies are recognized: semi-restricted subtidal, open-marine subtidal, and these are further subdivided into six and nine lithofacies in the Yuejin and Tuoputai area, respectively. In general, these facies are vertically arranged into shallowing-upward, meter-scale cycles. These cycles are commonly composed of a thinner basal horizon reflecting abrupt deepening, and a thicker upper succession showing gradual shallowing upwards. Based on the vertical facies arrangements and changes across boundary surfaces, two types of cycle: semi-restricted subtidal and open subtidal, are further identified. The semi-restricted subtidal cycles, predominating over the middle-upper Yingshan Group and the lower Yijianfang Group, commence with algal bindstone in the bottom and are capped by pelletoid grainstone and bindstone with peloidal grains. In contrast, the open subtidal cycles, dominating the upper Yijianfang Group, are dominated by clastizoic grainstone or clastizoic Bindstone. Based on vertical lithofacies variations, cycle stacking patterns, and accommodation variations revealed by Fischer plots, nine larger scale third-order depositional sequences (Sq3-Sq11) are recognized. These sequences generally consist of a lower transgressive and an upper regressive systems tract. The transgressive tracts are dominated by thicker than-average cycles, indicating an overall accommodation increase, whereas the regressive tracts are characterized by thinner-than-average cycles, indicating an overall accommodation decrease. The sequence boundaries are characterized by transitional zones of stacked thinner-than-average cycles, rather than by a single surface. These sequences can further be grouped into lower order sequence sets: the lower and upper sequence sets. The lower sequence set, including Sq3–Sq7, is at the rising–descending cycle in Fisher Curve plots. And this indicates the accommodation space keeps steady. The upper sequence set, including Sq8–Sq11, some features can be found that these Fisher Curves of sequences flunctuate strongly in the middle-lower Yijianafang Group while keep steady in the upper part. This indicates a phenomenon, where the accommodation space varies from violent to gentle.

Keywords Facies · Stratal cyclicity · Sequences · Lower-Middle Ordovician · Tarim Basin · China

Introduction

High-frequency meter-scale cycles are basic building units of shallow-water carbonate successions, which are commonly organized into larger scale depositional sequences. Many thick shallow-water carbonate successions are characterized by a clear hierarchical stratal cyclicity which is widely considered to having been driven by variable-order sea-level fluctuations (Fischer 1964; Goldhammer et al. 1990, 1993; Fischer and Bottjer 1991; Montanez and Osleger 1993; Mutti and Simo 1993; Strasser and Hillgartner 1998; Strasser et al. 2000; Chen et al. 2001; Hofmann et al.

Jiao Cun-Li and Zhao Xue-Qin contributed equally to this work.

✉ Cunli Jiao
1953394383@qq.com

[1] Research Institute of Exploration and Production, SINOPEC, Beijing 100083, China

[2] State Key Laboratory of Petroleum Resources and Prospecting, China University of Petroleum, Beijing 102200, China

2004; Hofmann and Keller 2006; Laya et al. 2013). Such stratal cyclicity in platform carbonates can be exhibited by the vertical cycle stacking patterns, which are commonly shown by the Fischer plot (Fischer 1964; Goldhammer et al. 1987; Read and Goldhammer 1988; Osleger and Read 1993; Chen et al. 2001; Chen and Tucker 2003). Many studies have documented the stratigraphy and sequences of Lower-Middle Ordovician shallow-water carbonate successions, such as those in Tarim Basin (Yu 1996; Qu, et al. 1997; Chen et al. 2003; Zhao et al. 2009; Hu et al. 2010; Wang et al. 2011; Wu et al. 2012; Wang 2013).

The Tarim Basin has been the important petroliferous basin in west China where a considerable quantity of commercial oil and gas has been discovered in the well Shacan 2 from Ordovician carbonates since 1984, and Lunnan-Tahe oil field has been built in Tabei uplift, which has about 1.5 billion tons reserve. Besides, carbonate oil and gas fields have been found in the lower Paleozoic in Tazhong uplift and Bachu uplift. It is a great challenge to establish an effective distribution model of reservoir in the study of carbonates (Lee 1997; Montanez 1997; Heasley et al. 2000; Hendry 2002; Tian et al. 2016, 2017; Lu et al. 2017). Thus it is critical to study the time and space sequences of the facies and its environment for carbonates (Vincent et al. 2007), and, therefore, we should focus on the composition, the spatial distribution characteristics of facies and environment, and analysis of time evolution sequence, which are especially important for carbonate reservoir and. Few studies have been carried out on the high-frequency, meter-scale cycles. This has resulted in many uncertainties in the identification of the larger scale depositional sequences of the platform carbonates and in our understanding of platform evolution.

This study aims to: (1) describe the lithofacies and meter-scale cycles in the Lower-Middle Ordovician Yingshan and Yijianfang Group in the Yuejin-Tuoputai Region, with a view to deduce the depositional environments; (2) illustrate the vertical cycle stacking patterns and hierarchy of stratal cyclicity using the graphic tool of Fischer plots; and (3) to determine the third-order sequences in the Yingshan and Yijianfang Group and their correlation with those in the coeval carbonate successions elsewhere around the world. This study could refine the time-stratigraphic framework for the Lower-Middle Ordovician, which is generally devoid of sufficient biostratigraphic controls in the Tarim Basin, and improve our understanding of carbonate platform evolution.

Geological setting

Tarim Basin, a big sedimentary basin, is located in the west of China,with a total area of 56×10^4 km^2. This Basin experienced a long geological evolution and multi-period tectonic events from Sinian to Neogene and was called a multi-cycle or superimposed basin. It stands between two giant mountains, Mt. Tianshan and Kunlun, and the eastern boundary is Altun Tagh fault zone. In Paleozoic, several paleo-uplifts and paleo-depressions developed in Tarim Basin. For instance, the main paleo-uplifts were Tazhong, Bachu, Tabei, and Taxinan uplift (He et al. 1996; Jia et al. 1997). Now, carbonate rocks are mainly distributed from Sinian to Lower Ordovician, showing diverse reservoir types and great reservoir property for oil and gas (He et al. 1996; Jia et al. 1997).

As shown in Fig. 1, Yuejin-Tuoputai area is located in the southwest of the Tahe, the north is Akkol bulge, which is located in the middle of Shaya uplift. Manjiaer Depression lies in the east, and Shuntuoguole uplift lies in the south. Tuoputai block is located in the northeast of the Yuejin block. Due to adjacence to Tahe area, there are a lot of similarities in tectonic evolution and distribution of fracture system. Therefore, a strong comparative research value in sedimentary, diagenetic and hydrocarbon accumulation is found between Yuejin-Tuoputai and Tahe. Under the control of complex and variable tectonic pressure field, Yuejin-Tuoputai area experienced a complicated evolutionary process (Xu et al. 2006). The Tabei uplift was in stable carbonate platform from late Sinian to Middle Ordovician, and until late Ordovician to Devonian, there was a weak tectonic uplift caused by the subduction of southern Kunlun. Meanwhile, the sedimentation continued. From late Devonian to early Carboniferous, influenced by the southern Tianshan activitty in the north basin, Tabei was uplifted strongly in general, and Silurian to the lower Ordovician stratums suffered various erosion. At the beginning of the Permian, with intense magmatic activity, the basin was in extensional tectonic activity period and with submersion generally. In early Permian period, the Tarim plate had collided with the West Kunlun plate and central Tianshan plate; Tabei intensively uplifted, and Permo-Carboniferous stratums were destroyed. In Meso-Cenozoic period, as Kuqa depression subsidence was aggravated, Tabei region became a remnant Paleozoic uplift, and Tahe and the adjacent area entered depositional stage of the inland depression basin. In late Tertiary period, strong subsidence took place in Tabei area caused by Xishan movement (Jia et al. 1997).

Ordovician strata are well developed in Yuejin-Tuoputai region; from base to top, the strata are Penglaiba Group in lower series of Ordovician, Yingshan Group in middle-lower series Ordovician, Yijianfang Group in middle series of Ordovician, Qrebake Group in upper series of Ordovician and Querquek Group. The middle–lower series of Ordovician are mainly developed Plateau facies such as gypsum dolomite, dolomite, limy dolomite and limestone. The upper series of Ordovician are mainly slope facies composed of limestone with mud and knollenkalk. However, the Querquek Group is dominated by clastic sedimentary of neritic shelf facies (Li et al. 2015).

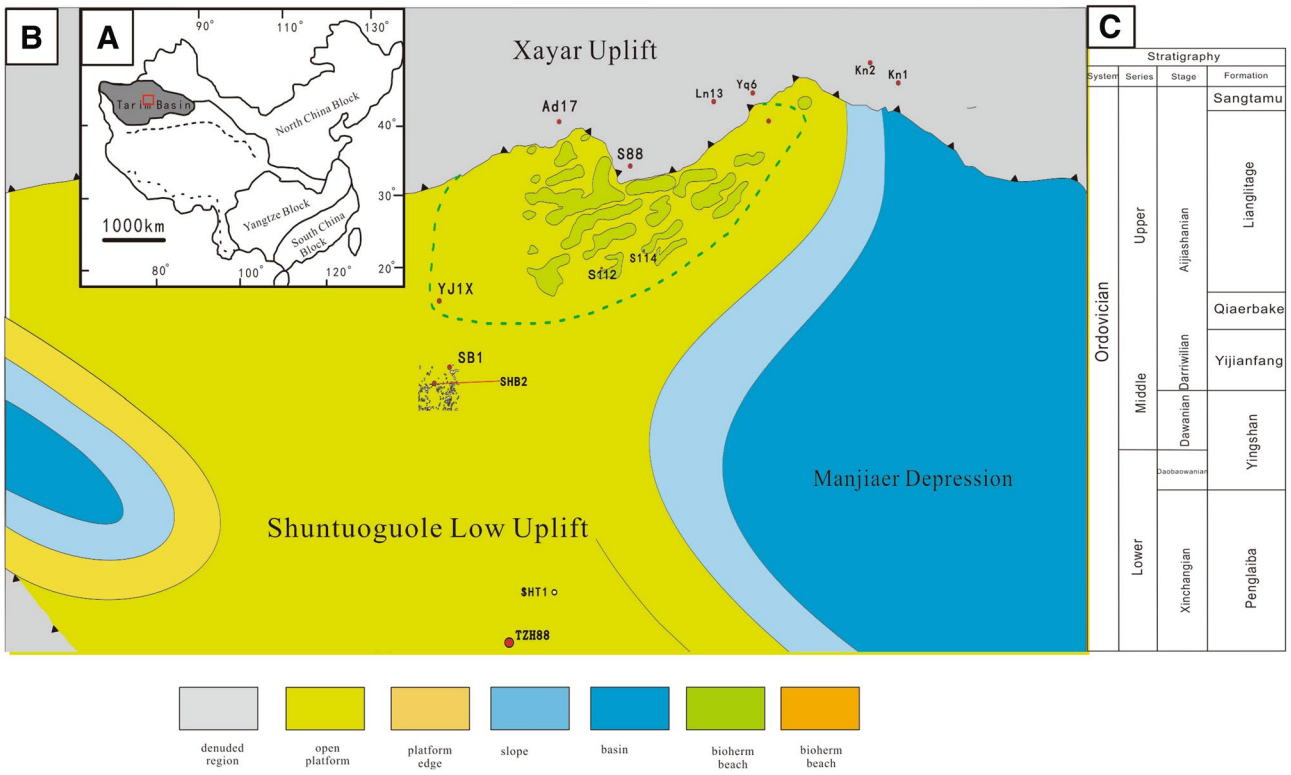

Fig. 1 **a** The schematic tectonic map of China and the position of Tarim basin. The red box indicates the position of 1B. **b** Sedimentary faces of Shuntuoguole area during Yijiangfan Group period. **c** Ordovician stratigraphy system of Shuntuoguole area

A set of marine carbonate rocks was deposited in the Upper Yingshan-Yijianfang group in Yuejin-Tuoputai region, with thicker and stable deposition. The environment is characterized an open platform, which can be subdivided into intraplatform shoal and interbank sea microfacies.

The development of the intraplatform shoal is controlled by local landforms and presents band distribution. In the Yingshan group period, the study area was in the open platform environment, but relatively limited, mainly developed dolomitized limestone or dolomite. In the early Yijianfang group, the open water was significantly enhanced and intraplatform shoal was expanded. The south of the study area mainly developed interbank sea microfacies and intraplatform shoal microfacies in the north. Sedimentary rocks were mainly composed of microcaystalline limestone, grainstone and biogenic limestone. In the later Yijianfang group, the study area was still an open platform, and the intraplatform shoal microfacie was expanded and patch reef was developed.

Materials and methods

Two Middle-Lower Ordovician borehole sections in Yuejin-Tuoputai area are the research objectives in this study, including YJ1X well located in Yuejin block and S114 well located in Tuoputai block.

YJ1X well, locating in Yuejin block, is sited in Xayar County. Yuejin block lies in the north of Shuntuoguole low uplift: the west is Yingmaili salient, the north is Halahatang depression and the east is Tuoputai block, the cored intervals are focused on Yingshan and Yijianfang Group, and total depth is from 7195 m to 7280 m. S114 well, locating in Tuoputai block, is sited in the southwest of Tahe. Tuoputai block is situated in the south of Akekule in the middle part of Xayar uplift, Tarim Basin. The target strata are the upper member of Yingshan and Yijianfang Group, the top depth of the former is 6422 m, the lower part is not drilled, and the latter lasts from 6319to 6422 m.

The lithofacies of the Yingshan and Yijianfang Group were described and interpreted in terms of lithology, textures/fabrics, sedimentary structures, bed geometry and color. Hundreds of standard thin-sections from hand samples were prepared for petrographic studies. The terminology employed in description, in principle, followed the carbonate classification of Dunham (1962).

Depositional facies (or environments) were identified and interpreted based on the tempo-spatial relationship and similarity of the lithofacies' association described with regard to well-proven diagnostic sedimentary characteristics. High-frequency, meter-scale cycles were identified mainly based on the recurrences of vertically stacked

lithofacies (or facies) and their transitional (gradual or abrupt) patterns across the bounding surfaces.

Fischer plots were applied to illustrate vertical cycle stacking patterns and long-term changes in accommodation space on carbonate platforms (Fischer 1964; Sadler et al. 1993; Bosence et al. 2009). Based on the assumed or determined average periodic value of meter-scale cycles, Fischer takes time as *X* axis and cumulative thickness of meter-scale cyclic-sequences belong to peritidal type as *Y* axis, which has taken liner settlement correction, and thus a diagram is obtained.

Osleger pointed out that the each cycle time is variable and the loss of cycle is common in sections. Therefore, using the number of cycles as *X* axis instead of time could avoid the limitation of Fischer application.

Reed thought that it was not very strict for taking "cumulative thickness" as *Y* axis, Therefore, it was emphasized that the so-called cumulative thickness was corrected by linear settlement. The subsidence history of basin is very complex, so the subsidence process of the basin during the group of each meter-scale cycles is difficult to grasp.

The cumulative thickness of meter-scale cyclic-sequences under liner settlement correction by Reed is "accumulation offset of average thickness" in deed, which is the accumulation difference between the thickness of every cycle and the average thickness of all cycles and represents the *Y* axis instead of original ordinate. When drawing the Fischer diagram, the *X* axis is the number of cycles, and the *Y* axis is the cumulative thickness of the average thickness, that is, the offset accumulation of the thickness of all meter cycles to the average cycle thickness. In Fischer diagram, the connection of the vertex coordinates of each cycle is cumulative offset curve of average thickness with cyclic number as a function, which represents the variation of effective accommodating space in the group of sediment. Therefore, the Fischer diagram is also known as the new accommodating space diagram, which is an important way to study the superposition rule of sedimentary cycle in space, relative sea level change, cycle order and cyclic stratigraphic correlation.

Larger-scale third-order sequences were determined based on the cycle stacking patterns and accommodation changes revealed by the Fischer plots, together with facies stacking patterns (i.e., fresh water solution seam and mold pore in each cycle) and depositional indicators.

Depositional facies

Six and nine lithofacies (LY1–LY6 and LT1–LT9, respectively) were identified in the Yingshan and Yijianfang Group. These lithofacies can be further categorized into several facies associations, representing various depositional environments, such as intertidal, semi-restricted subtidal, and open-marine subtidal (Tables 1 and 2, Figs. 2, 3 and 4).

Semi-restricted subtidal zone (YJ1X)

Bindstone (LY1): The main structure of the rock is bindstone, Girvanella algae mycelium might be observed occasionally, and bioturbate texture and granule are visible partly. In these sediments, grains and bind-structure could not be distinguished easily and the original structure is hardly identified. In addition, trilobites and ostracodas might be observed occasionally. The pyrite can be seen commonly in the rocks. Sparry cement usually has four occurrences. The first is blocklike sparry cement, which transits sharply from algae binder, is presumed to form in early diagenesis stage. However, Yinxue Han et al. (2015) regarded it as a result of microcrystalline calcite caused by neomorphism, the crystal, mosaic-like if contacted,is dirty and matrix limestone remained; The second is cement filling fractures, which is the same occurrence as cements in pores. The third is pelletoid intergranular cement. It is usually small, and this kind of cement has the lowest content because the particles are relatively rare. The fourth is poikilotopic calcite in bioturbation place. The crystal is clean, a few particles suspended by basal cemented, and frosting phenomenon can be found under orthogonal light. This kind of cement contains a small amount of liquid single-phase inclusion while under 500 times magnification, indicating the calcite was formed in the early low-temperature environment. The absence of biogenic debris and fenestrate hole illustrates that the environment is semi-restricted deep-water subtidal zone.

Clastizoic bindstone (LY2): The main structure of the rock is bindstone. No sparry cement can be found compared with LY1. Biogenic debris takes over 20–70% of the whole sediments, mainly consisting of trolibites and echinoderms with micritization commonly. Its grain diameter is less than 500 μm, and of medium-sorting and stacked in disorder. The intergranular is filled with algae mycelium and algae binding. Generally, the existence of massive echinoderms debris indicates 2 types of environment. One is back reef zone with moderate hydrodynamic environment. The other is internal-medium gentle slope with deeper and lower energy environment. Cause reef is not developed in Yuejin area; the rocks can be suspected as forming in the open middle-deep subtidal environment.

Clastizoic Bindstone with peloidal grains (LY3): the content of biogenic debris is less than 10% in general, mainly consisting of brachiopods and echinoderms. The main structure of the rock is bindstone, which takes over more than 40% of the whole sediments. The grains are mainly consisted of pelletoid and peloidal grainstone with algae, what's more, the content of grains is lower and less than 35%. The degree of sorting and roundness is poor and the

Table 1 Lithology types of Yuejin area

Facies	Lithology type	Description	Fossile	Environment Interpretation
Semi-restricted subtidal zone	Bindstone (LY1)	The main structure of the rock is bindstone, Girvanella algae mycelium might be observed occasionally, and bioturbate texture and granule are visible partly.In these sediments, grains and bind-structure could not be distinguished easily and the original structure is hardly identified.Sparry cement are well developed	Trilobites and ostracodas are incidental	Semi-restricted deep-water subtidal zone
Open-marine subtidal zone	Clastizoic bindstone (LY2)	The main structure of the rock is bindstone, the content of biogentic debris is high. No sparry cement It's grain diameter is less than 500um, and it's of medium-sorting and stacked in disorder. The intergranular is filled with algae mycelium and algae binding	Biogenic debris takes over 20–70% of the whole sediments, and trolibites and echinoderms with micritization are common	Open middle-deep water subtidal environment
	Clastizoic Bindstone with peloidal grain (LY3)	The main structure of the rock is bindstone, The grains are mainly consisted of pelletoids and peloidal grainstone with algae chipping.the content of grains is lower and less than 35%, the grain diameter is between 100 and 200um and the degree of sorting and roundness is poor.It has a small number of dissolved pores. Interparticle sparry cement are developed	The content of biogenic debris is less than 10%, and brachiopods and echinoderms are common	Open middle-deep water subtidalzone
	Pelletoid Grainstone with bound structure and clastizoic (LY4)	The grains are mainly consisted of pelletoids (more than 70%). Its grain diameter ranges from 100 to 200um and the degree of sorting and roundness is medium. The bind-structure can be observed locally, and interparticle is mainly filled with poikilitic cements and no pores	The content of biogenic debris is about 20%, brachiopod and echinoderms are common	Open shallow-water subtidal zone
	Pebbled Grainstone with bound structure and clastizoic (LY5)	The sedimentary environment of this lithology is almost the same to LY4.The content of grains is about 60%. This kind of rock contains more gravel grains, alike intraclast. And the degree of roundness is very poor, the interparticle sparry cement is mainly consisted of calcsparite and there are more intensive suture lines. It is likely to indicate a higher content of matrixand a deeper water condition than LY4	Brachiopod and echinoderms are common	Open middle-water subtidal zone
	Clastizoic Grainstone (LY6)	The structure of the rock is grain-supported and the grains are mainly consisted of pelletoids (about 55%) and biogenic debris, grain diameter is more than 150 μm, and the degree of sorting and roundness is poor, the interparticle sparry cement is mainly consisted of granulated or massive calcsparite	The biogenic debris is(about 20%) mainly consisted of brachiopods, echinoderms debris and bryozoan	Open shallow-water subtidalzone

Table 2 Lithology types of southern Tuoputai area

Facies	Lithology type	Description	Fossile	Environment Interpretation
Mi-restricted subtidal z	Pelletoid Grainstone (LT1)	The content of alga chipping is more than 65% and its grain diameter is kind of big (more than 100 μm). Also a small amout of aedelite is contained and the diameter is more than 2000 μm. Freshwater dissolved fracture can be often found in this kind of rock	No biogenic debris	Semi-restricted shallow-water subtidal environment
	Pelletoid Grainstone with bound structure (LT2)	The content of grain is between 50 and 65%. Its grain diameter ranges from 60 to 150um. The content of biogentic debris is very low and the prehnite (grain diameter: 1–2 mm) are common. Typical bioturbation can be observed in which poikilitic calcite exist, while the particles are basal cement	Trolibites and echinoderm are common	Semi-restricted shallow-middle water subtidal zone
	Bindstone with Peloidal grains (LT3)	Bind-structure is the main, the bioturbation structure usually develops well in this lithology.The content of pelletoid is between 10 and 50%. Its grain diameter ranges from 60 to 100 μm. The content of biogenic debris is very low (less than 1%), pyrite is incidental	Ostracoda, trolibites, gastropod and brachiopod are common	Semi-restricted middle-deep water subtidal zone
	Bindstone (LT4)	The main structure of the rock is bindstone, Girvanella algae mycelium might be observed occasionally, and bioturbate texture and granule are visible partly. Grains and bind-structure could not be distinguished easily and pyrite is incidental	Brachiopods and echinoderm debris are incidental	Semi-restricted deep water subtidal zone
	Clastizoic Bindstone with peloids (LT5)	The sedimentary environment of this rock is similar with LT3,the difference The differences are that the rocks here have certain biogenic debris,which indicating a more open water body.This lithology is commonly located in the transition between semi-restricted environment and open shallow water subtidal environment	Echinoderm and brachiopod are common	Semi-restricted deep-water subtidal zone
Open subtidal zone	Oosparite (LT6)	The structure of the rock is grain-supported and the grains are mainly consisted of ooid (more than 70%), its grain diameter ranges from 200 to 300um, Concentric lamina can be seen inside of ooid, instead of radial structure. Girvanella algae mycelium and moldic pore are incidental	No biogenic debris	Open shallow water tidal zone
	Clastizoic Oosparite (LT7)	The sedimentary environment of this rock is between LT6 and LT7		Open shallow-water subtidal zone
	Clastizoic Grainstone (LT8)	The structure of the rock is grain-supported and the grains, which takes over more than 70% of the whole sediments and its grain diameter ranges from 200 to 500um. There is a strong micritization in the peripheral of biogenic debris. Massive calcsparite is filled in intergranular	Echinoderm debris are common	Open shallow-water subtidal zone
	Clastizoic bindstone (LT9)	The main structure of the rock is bindstonemost of which have micritization and stacked in disorder. The diameter of debris usually less than 500 μm. The degree of sorting is medium The intergranular is filled with algae mycelium and algae binding	The content of biogentic debris is very high (35% to 65%) echinoderms are common	Open middle-deep water subtidal zone

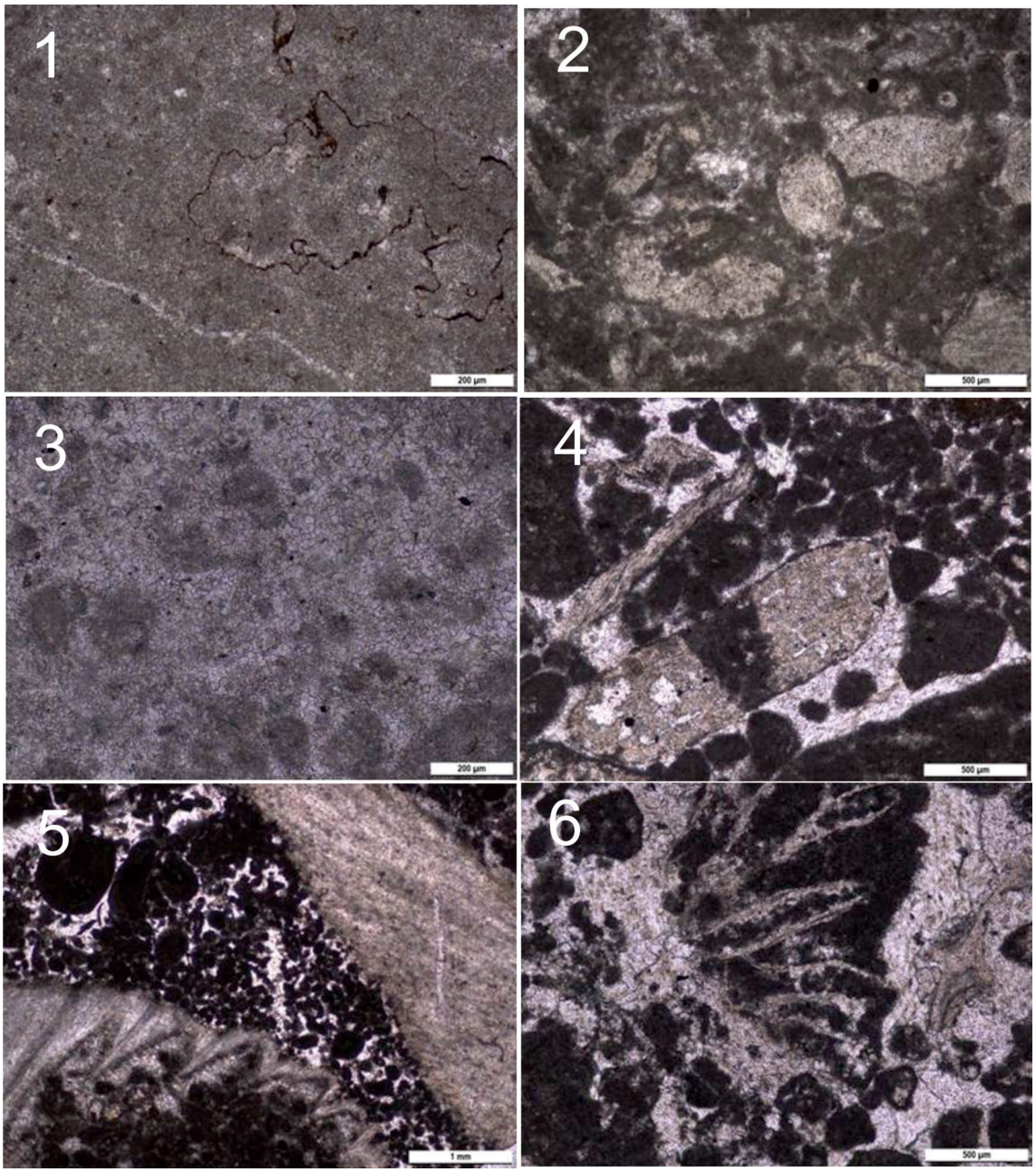

Fig. 2 Lower-Middle Ordovician Lithology microfacies of Yuejin area. Introduction: 1. LY1—bindstone, YJ1X well, 7274.19 m; 2. LY2—clastizoic bindstone, YJ1X well, 7201.77 m; 3. LY3—clastizoic bindstone with peloidal grains, YJ1X well, 7270.14 m; 4. LY4—pelletoid grainstone with bound structure and clastizoic, YJ1X well, 7258.56 m; 5. LY5—pebbled grainstone with bound structure and clastizoic, YJ1X well, 7263.97 m; 6. LY6—clastizoic grainstone, YJ1X well, 7257.50 m

grain diameter is between 100 and 200um. It has a small number of dissolved pores. There are two types of the calcsparite, One is flaky or small-size bulk calcite which grows in bioturbation place. The crystal is dirty, which is around 50um and mosaic-likeof contacted. The other is interparticle sparry cement, granular, which is less than 20um of diameter generally and mosaic-likeof or embayed contacted. The echinoderms debris usually has a phenomenon of siliceous metasomatosis. Obviously, its sedimentary environment is between the one of grainstone and the one of bindstone, and the significant increase of biogenic debris indicates that the environment is slightly open. So it is assumed to be open middle-deep water subtidal environment, above storm wave base.

Pelletoid Grainstone with bound structure and clastizoic (LY4): The content of biogenic debris is about 20%, mainly

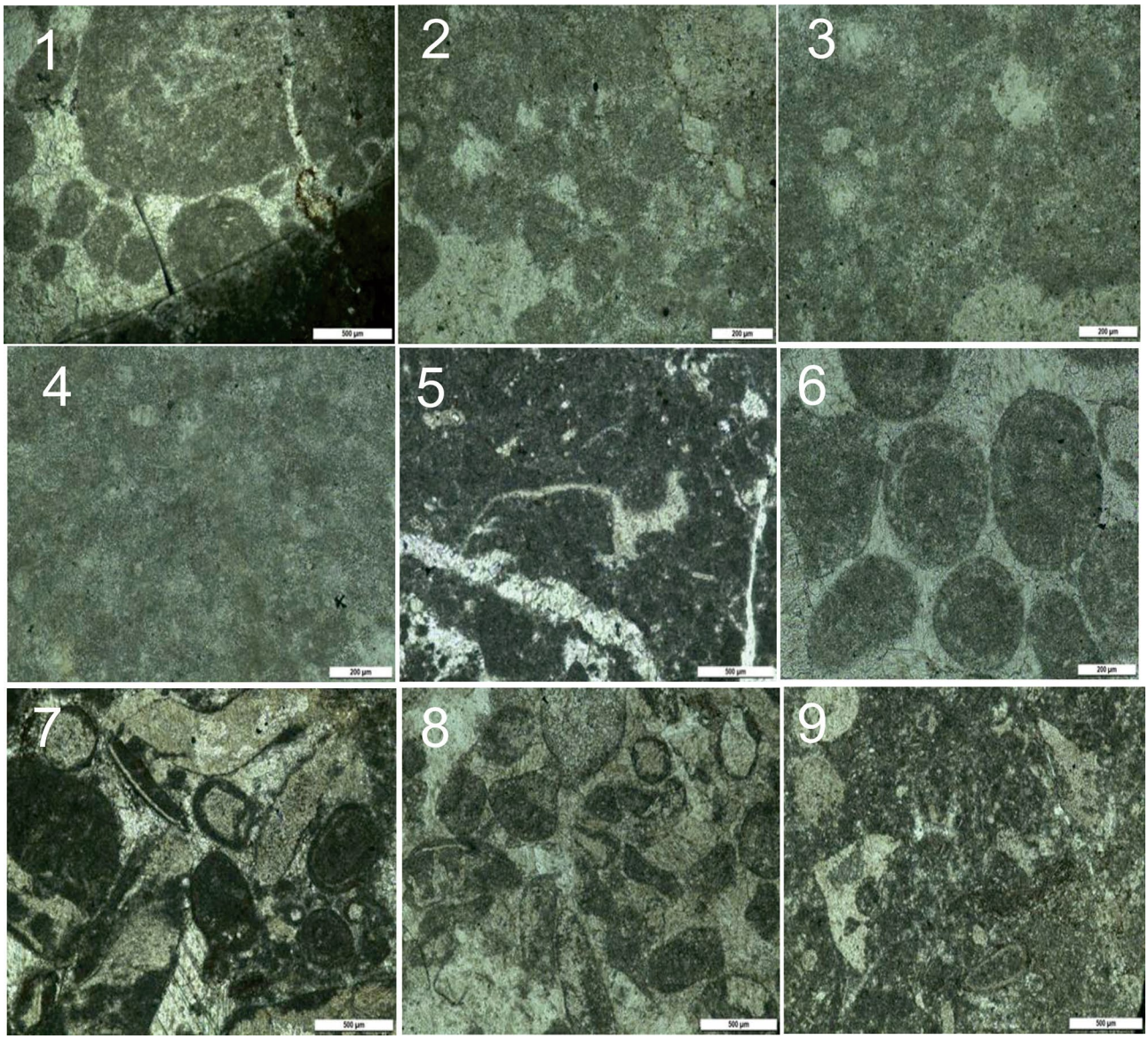

Fig. 3 Lower-Middle Ordovician Lithology microfacies of Tuoputai area. Introduction: 1. LT1—pelletoid grainstone, S114 well, 6398.5 m; 2. LT2—pelletoid grainstone with bound structure, S114 well, 6405.5 m; 3. LT3—bindstone with peloidal grains, S114 well, 6383.5 m; 4. LT4—bindstone, S114 well, 6373.5 m; 5. LT5—clastizoic bindstone with peloids, S114 well, 6370.5 m; 6. LT6—oosparite, S114 well, 6349.5 m; 7. LT7—clastizoic oosparite, S114 well, 6346.5 m.8. LT8—clastizoic grainstone, S114 well, 6343.5 m; 9. LT9—clastizoic bindstone, S114 well, 6331.5 m

consisting of brachiopods and echinoderms. Its grain diameter is a little big and well preserved. The grains are mainly consisted of pelletoid, which takes over more than 70% of the whole sediments. Its grain diameter ranges from 100 to 200um and the degree of sorting and roundness is medium. The bind-structure can be observed locally, and interparticle is mainly filled with poikilitic cements and no pores. Both the obvious increase of grains and the higher content of biogenic debris indicate the rocks formed in the open shallow-water subtidal zone with stronger hydropower under the normal wave base.

Pebbled Grainstone with bound structure and clastizoic(LY5): Compared to LY4, the lithology is almost the same, while there are four main differences. First, this kind of rock contains more gravel grains, alike intraclast. And the degree of roundness is very poor, which indicating an episodic strong hydrodynamic environment, maybe affected by storm. Second, it has a lower content of grains, which is about 60%, suggesting that the hydrodynamic is weaker compared with LY4 and maybe located in deeper part of plateau. Third, the interparticle sparry cement mainly consists of calcsparite. And forth, there are more intensive

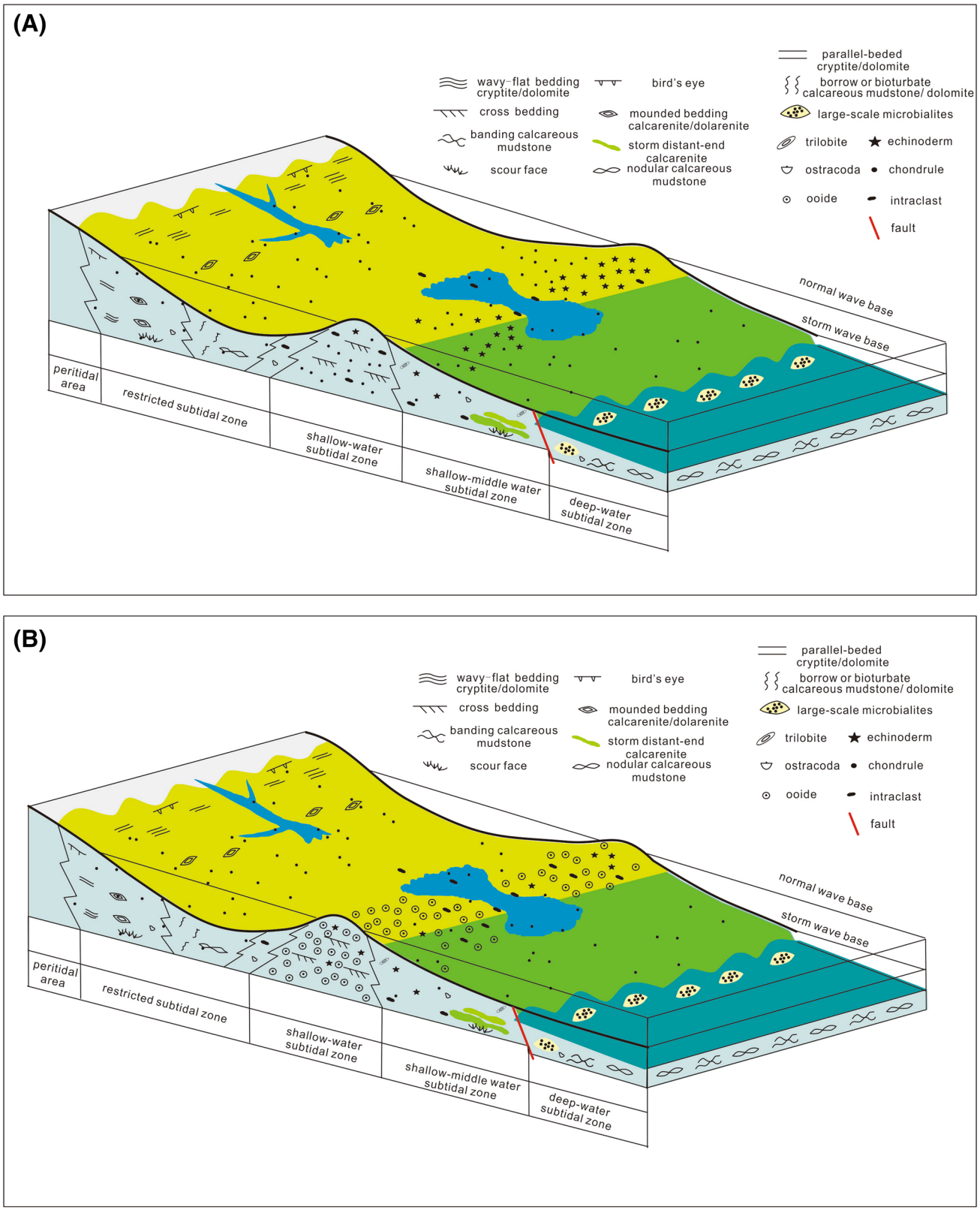

Fig. 4 **a** Lower-middle Ordovician Yingshan-Yijianfang Group Paleogeographic map of Yuejin area. **b** Lower-Middle Ordovician Yingshan-Yijianfang Group Paleogeographic map of Tuoputai area

suture lines. It is likely to indicate a higher content of matrix and a deeper water condition than LY4. Above all, The rocks can be suspected as forming in the open middle-water subtidal zone, located above storm wave base.

Clastizoic Grainstone (LY6): The structure of the rock is grain-supported and the grains mainly consist of pelletoid and biogenic debris. Biogenic debris takes over 20% of the whole sediments while pelletoid accounts for 55% on the whole, and its grain diameter is more than 150 μm. The interparticle sparry cement mainly consists of granulated or massive calcsparite. The biogenic debris mainly consists of brachiopods, echinoderms debris and bryozoans. And the degree of sorting and roundness is poor. The high content of Biogenic debris and the overall structure of the rock show an open shallow-water subtidal environment, which is near the normal wave base, and represents the shallowest sedimentary environment of Yuejin area.

Semi-restricted subtidal zone (S114)

Pelletoid Grainstone (LT1): The content of alga chipping is more than 65% and its grain diameter is kind of big (more than 100 μm). Also a small amout of aedelite is contained and the diameter is more than 2000 μm. There is no biogenic debris. Two kinds of sparry cement are developed around the grains. The first phase is small-size irregular-shape calcite which grows around the grain, and the other is blocklike sparry cement closer to the center of the intergranular pore which is suspected as a synchronous product with the former one and needed to be proved by cathodeluminescence test. Its pore is very poor. However, Asphalt is filled in the intergranular and intercrystal pores of calcite cement, which shows that micropores are well developed and can be used as reservoir space of oil and gas. Freshwater-dissolved fracture can be often found in this kind of rock, indicating that the rock may be exposed to freshwater in very shallow water, usually at the top of the cycle. The existence of aedelite and pelletoid and the absence of the wide sea creatures illustrate that the environment is semi-restricted environment. Also the low content of algae binding component shows a shallow water with strong hydrodynamic, which is under the normal wave base.

Pelletoid Grainstone with bound structure (LT2): The content of grain is between 50 and 65%. Its grain diameter ranges from 60 to 150 μm. The prehnite(grain diameter: 1–2 mm) are also very common in the rocks, while only a small amount of biogenic debris can be seen and it is mainly composed by trolibites and echinoderms. Typical bioturbation can be observed in which poikilitic calcite exists, while the particles are basal cement. The common intergranular sparry cements are similar to pelletoid grainstone (LT1). Then, its sedimentary environment is between pelletoid grainstone(LT1) and bindstone with peloidal grains (LT3), and might be semi-restricted shallow-middle water subtidal zone.

Bindstone with Peloidal grains (LT3): The bioturbation structure usually develops well in this lithology. The content of pelletoid is between 10 and 50%. Its grain diameter ranges from 60 to 100 μm. The pyrite can be seen occasionally in the rocks. While only a small amount of biogenic debris(less than 1%) can be seen and is mainly composed by ostracodas, trolibites,gastropods and brachiopods. The bind-structure has the biggest proportion as a whole. Additionally, the content of biogenic debris and grains is extremely low. Thus, the sedimentary environment can be inferred as semi-restricted middle-deep water subtidal zone. What is more, the existence of bioturbation structure and the absence of the influence from storm illustrate that the environment is under the storm wave base.

Bindstone (LT4): The main structure of the rock is bindstone, Girvanella algae mycelium might be observed occasionally, and bioturbate texture and granule are visible partly. In these sediments, grains and bind-structure could not be distinguished easily and the original structure is hardly identified. In addition, trilobite, brachiopods and echinoderm debris might be observed occasionally. The pyrite can be seen commonly in the rocks. Sparry cement usually is of two types. One is pelletoid intergranular cement. It is usually small, and this kind of cement has the lowest content because the particles are relatively rare. The other is poikilotopic calcite in bioturbation place. The crystal is clean, a few particles suspended by basal cemented, and frosting phenomenon can be found under orthogonal light. This kind of cement contains a small amount of liquid single-phase inclusion while under 500 times magnification, indicating the calcite was formed in the early low-temperature environment. Therefore, represents semi-restricted deep water subtidal zone.

Clastizoic Bindstone with peloids (LT5): The sedimentary environment of this rock is similar to bindstone with peloidal grains (LT3)'s. The difference is that this kind of rock has a certain amount of biogenic debris, mainly consisting of echinoderms and brachiopods, which indicates a more open water environment. This lithology is commonly located in the transition between semi-restricted environment and open shallow water subtidal environment, so we suspect that it develops from the semi-restricted deep-water subtidal zone instead of open deep water subtidal zone.

Open subtidal zone (S114)

Oosparite(LT6): The structure of the rock is grain-supported and the grains mainly consist of ooid. Ooid takes over more than 70% of the whole sediments and its grain diameter ranges from 200 to 300um. Concentric lamina can be seen inside of ooid instead of radial structure. Two kinds of sparry

cement are developed around the grains. The first phase is isopachous and rim bladed calcite which grows around the ooid, and the other is blocklike sparry calcite close to the center of the intergranular pore. Girvanella algae mycelium and moldic pore might be observed occasionally. The oosparite is the typical rock type of the open shallow water tidal zone. Therefore, we suspect that it develops from the open shallow-water subtidal and above normal wave base.

Clastizoic Oosparite (LT7): The sedimentary environment is between oosparite(LT6) and clastizoic grainstone(LT8)s, which is located in open shallow-water subtidal zone and near normal wave base.

Clastizoic Grainstone (LT8): The structure of the rock is grain-supported and the grains mainly consist of echinoderm debris, which takes over more than 70% of the whole sediments and its grain diameter ranges from 200 to 500um. There is a strong micritization in the peripheral of biogenic debris. The sparry cement presents massive calcsparite, the diameter of which gradually increases towards pore center. Also, clastizoic grainstone, which is usually formed in deeper water than oosparite, is the typical rock type of open shallow tidal zone where hydropower weakens and good transmittance and high oxygen contents display. So we conclude that it develops from the open shallow-water subtidal zone and under normal wave base.

Clastizoic Bindstone (LT9): The main structure of the rock is bindstone, which is characterized by high content of biogenic debris. And the range is from 35 to 65%. Biogenic debris mainly consists of echinoderms, most of which have micritization and are stacked in disorder. The diameter of debris usually is less than 500 μm. The degree of sorting is medium. The intergranular are filled with algae mycelium and algae binding. Generally, the rocks can be explained as forming in the open middle-deep water subtidal zone compared to Yuejin area.

High-frequency meter-scale cycles

The sedimentary microfacies identification results of YJ1X well and S114 well are marked on the histogram (Fig.). It is obvious that the carbonate sediments show apparent cyclonic accumulation characteristics. That is on the meter-scale; the sedimentary microfacies are not always invariable, and always appear repeatedly in accordance with a certain rule, indicating the repeated changes in the depth of the water body.

Actually, the Yingshan and Yijianfang Group is characterized by repeated shallowing-upward, meter-scale cycles.

Shallow subtidal facies through deep subtidal facies are organized into meter-scale, upward-shallowing cycles averaging 1.5–3 m thick, lasting 20-S100 kyr. Cycle boundaries vary from abrupt to transitional.

Based on the intracycle facies arrangement and features of the bounding surfaces, two dominant types of cycle are distinguished: semi-closed restricted subtidal and open subtidal.

The semi-closed restricted subtidal cycles are capped by semi-closed restricted subtidal facies, and these are dominan in the upper part of Yingshan Group and lower-middle part of the Yijianfang Group. In contrast, open subtidal cycles are capped by open subtidal facies, and mainly occur in the upper part of the Yijianfang Group.

The semi-restricted subtidal cycles are mainly composed of the lithology from semi-restricted shallow-deep subtidal zone, developing in the upper part of Yingshan Group and the lower part of Yijianfang Group. This type of cycle represents a regression association which is the transition from semi-restricted middle-deep subtidal lithology to the one of the semi-restricted shallow-water subtidal and deep-water intertidal zone. Exposure indicator cannot be found in the top of the cycle, which suggests an incomplete accumulation of accommodation space. Based on the types of diagenetic facies and their vertical superposition, these cycles can be divided into two types: (1) cycle with LT1 on the top and LT2-1T4 on the bottom, and (2) cycle with LT3 on the top and LT4 on the bottom.

(1) This kind of cycle starts from LT2 to LT4, which forms in the low-power semi-restricted intertidal zone and deep-water subtidal zone, and then changes upward into LT1, which develops in the more powerful semi-restricted shallow-water subtidal zone, ranging roughly between normal and storm wave base. The cycle does not accrete to the peritidal zone, which might be caused by storm erosion or the balance between sediments and accommodation space (Bádenas et al. 2005; Bádenas and Aurell 2010; Laya et al. 2013). Then, another reason might be that the growth rate of the accommodation space is higher than the production rate of sediments (Chen et al. 2001; Hamon and Merzeraud, 2008).

(2) This kind of cycle starts from the LT4, which forms in the low-power semi-restricted intertidal zone and deep-water subtidal zone, and then changes upward into LT3, which develops in the more powerful semi-restricted medium-depth water subtidal zone, locating roughly above storm wave base. The difference between this cycle and the one mentioned above is that there is almost no pelletoid here and the main structure is bondstone, which indicates a deeper water body.

The open subtidal cycle mainly consists of the lower open middle-deep water subtidal lithology and the upper open shallow-middle subtidal lithology, and it is also an incomplete regression cycle. In the sedimentary process, the sea-level fluctuation was so slight that it could not make the bottom of the sea exposed, so air exposure indicator (e.g. mud

crack and small tepee structure) did not develop in this kind of cycle. These upward shallowing meter-scale cycles have a fine continuity in horizontal direction and minor changes in thickness, but interfaces are almost discontinuous. Based on the types of diagenetic facies and their vertical superposition, five kinds of cycle can be identified, appearing in Yuejin area. Based on the depth of water, from deep to shallow, cycle is in sequence of LY6, LY5, LY4, LY3, and LY2 on the top. Two types of cycle can be identified in Tuoputai area: cycle with LT8 on the top and cycle with LT9 on the top. These cycles of open subtidal facies mainly develop in the upper part of Yijianfang Group in Yuejin-Tuoputai area, which can be roughly divided into two types. First, the cycle does accrete to the shallow-middle subtidal zone, which starts from the low-power open middle-deep water intertidal zone (such as LT9, LY2,etc.) and then changes upward into high-power shallow-middle water intertidal zone (such as LY6, LT8,etc.); the second type of cycle is dominated by bindstone, which is formed in middle-deep water subtidal environment. The content of biogenic debris is influenced by hydropower. At intracycle, from the bottom to the top, the content of biogenic debris increases and the diameter of grains is bigger, such as cycle with LT9 and LY2 on the top. In the Yijianfang Group in Yuejin-Tuoputai area, the peritidal lithology did not develop well, which could be represented by the evidence that the balancing effect between the increasing of accommodation space and the supply of sediments hardly made the sea-bottom accrete completely from sutidal zone to peritidal zone (Goldhammer et al. 1990; Elrick and Read, 1991; Elrick, 1995; Chen et al. 2001; Bádenas and Aurell 2010; Tucker and Garland 2010; Bayet-Goll et al. 2014).

It is difficult to determine cycle duration from thick platform carbonate successions as a result of lack of accurate radiometric age data and the `missed beat effect'. Here only an approximate estimation of cycle duration can be made with the given time-scale of the Floian, Dapingian and Darriwilian. If the deposits in the Floian and Dapingian are taken as a whole, the cycle duration is in the range 35.7 ~ 97.2 kyr (Guo 2010). If `missed beats' (deep subtidal missed beats) are taken into account, the cycle durations would be shorter than these estimated values. For most meter-scale carbonate cycles, these Ordovician ones are within the Milankovitch band, corresponding to fourth-and fifth-order cycles (cf. Goldhammer et al. 1993).

The origin of meter-scale, carbonate cycles is still a controversial topic, provoking much debate (e.g. Drummond and Wilkinson Goldhammer et al. 1993; Wilkinson et al. 1996, 1997). Three mechanisms are commonly

cited to explain the repetition: (1) autocyclic generation (e.g. Pratt and James 1986; Cloyd et al. 1990; Satterley 1996), (2) episodic subsidence (e.g. Cisne 1986; Hardie et al. 1991), and (3) high-frequency glacio-eustatic fluctuations in sea-level (e.g. Goodwin and Anderson 1985; Goldhammer et al. 1990, 1993; Balog et al. 1997; Strasser and HillgaÈrtner 1998).

The asymmetric cycles are dominant in the study area, the subtidal cycle with the top of the subtidal rock facies for example. The thickness of upper and lower part is 15% and 85%, respectively for the entire cycle, which corresponds to the rhythm of the change of the sea level fluctuation with track driven (Koerschner and Read 1989; Osleger and Read 1991; Goldhammer et al. 1993; Chen et al. 2001). It indicates that these cycles in study area should or at least largely be attributed to the high-frequency sea-level fluctuations of orbit driven. The most important thing is that the high-frequency, glacio-eustatic fluctuations in sea-level mechanism can explain all the subtidal cycles better. The lower part of subtidal cycles formed in the rising period of high-frequency sea level, and then the sea level remains at high position or slightly lower. In the high portions of terrain, such as the peritidal area and the edge of the platform, the tidal flat sedimentation progrades towards the sea direction and superimposed on the subtidal sediments. However, for deep water environment, the decline of sea level and the accumulation of sediments are not enough to make the seafloor accretion to the tidal flat area. Thus the shallow-water subtidal sediments are accumulated, which form a subtidal cycle that is not completely shallow. (Goldhammer et al.1990, 1993; Elrick 1995; Chen et al. 2001). The autocyclic generation and episodic subsidence clearly fail to explain the subtidal cycle in the region, for which the reasons are: (1) the episodic subsidence will produce abrupt lithofacies superposition pattern, which is obviously inconsistent with the gradient superposition pattern of the subtidal cycle; (2) the Tarim Basin is a passive continental margin basin in the middle lower Ordovician, and it is not possible to have such repeated pulse tectonic movement; (3) the thickness of the stratum is stable and transversely continuous; (4) the variation of the lithofacies is gradual and breccia accumulation during synsedimentary fault activity period has not been seen.

Vertical stacking patterns and depositional sequences

Cycle stacking patterns and accommodation change

In shallow-water carbonate successions, the thickness of cycles, particularly of peritidal cycles, generally reflect the change in accommodation space available during a eustatic fluctuation cycle (Fischer 1964; Goldhammer et al. 1987; Read and Goldhammer 1988). Although the relationship is complicated by many factors such as quasi-periodicity of cycles, variable sedimentation rates, incomplete

shallowing to sea level, non-linear subsidence rates, and 'missed beats' of sea-level change, these negative effects can be mitigated if additional information is included. Many studies have

shown that the stacking patterns of meter-scale cycles (i.e., stratigraphic trends in cycle thickness and facies variations) in platform carbonate successions are a good reflection of variable-order stratal cyclicity controlled by high-frequency accommodation fluctuations superimposed on long-term accommodation changes (Goldhammer et al. 1990, 1993; Osleger and Read 1991; Montanez and Osleger 1993; Chen et al. 2001; Schlager 2005; Tucker and Garland 2010). These attributes bridge the link of individual meter-scale cycles to larger-scale depositional sequences (tens to hundreds of meters thick). Thus the cycle stacking patterns, including facies stacking patterns, can be used to identify larger scale depositional sequences and their component systems tracts, especially in areas where the strata have been structurally deformed and are difficult to trace laterally.

The Fischer plot has been widely used as a graphical method to illustrate long-term accommodation changes by graphing cumulative departures from the mean cycle thickness as a function of time or cycle number (Fischer 1964; Goldhammer et al. 1987; Read and Goldhammer 1988; Sadler et al. 1993; Husineca et al. 2008; Bosence et al. 2009). A minimum of 50 cycles is recommended for this data analysis. In such a plot, thick cycle packages deviate positively from the mean cycle thickness, creating a rising limb of plots as a reflection of progressive increases in accommodation space during a relative sea-level rise. By contrast, thin cycle packages deviate negatively from the mean cycle thickness, producing a falling limb as a reflection of progressive decreases in accommodation space during the relative sea-level fall. In shallow water carbonates with poor biostratigraphical controls, the Fischer plot thus provides a useful tool to correlate the enormously thick shallow-water carbonate successions at different widely spaced sections, mainly based on the patterns of long-term accommodation changes (or sea-level changes), with additional information including facies stacking patterns, some specific facies indicators and stratigraphic marker beds, integrated to constrain the correlations (Adams and Grotzinger 1996; Bosence et al. 2000; Chen et al. 2001).

In this study, Fischer plots are constructed by graphing cumulative departures from the mean cycle thickness against cycle thickness rather than mean cycle duration or cycle number (Chen et al. 2001). In this objective way, the Fischer plots produce similar accommodation fluctuation curves but with a more gently rising limb and steeper falling limb. Based on the previous analysis of facies, the shallow water subtidal environment and middle-deep water subtidal zone are in intercalary development in Yijianfang Group in well YJ1X, while the shallow-water subtidal cycles in upper part of Yinshan Group and the middle-lower part of Yijianfang Group are developed, and the upper part of Yijianfang Group is mainly deep water subtidal. In view of the dominance of medium-to deeper-water subtidal cycles in the studied Group, the effects of 'missed beats' of low-amplitude, high-frequency sea-level fluctuations in deep subtidal environments (Osleger and Read 1991; Sadler et al. 1993) are likely to be minor.

Third-order depositional sequences

The sequence boundary surface, as indicated by long-term subaerial exposure (i.e., karstification, pedogenesis) and/or large-scale downward incision, is the key to demarcate the third-order depositional sequences (Van Wagoner et al. 1995; Vail et al. 1991; Schlager 2005). In the study area, however, the sequence boundaries are indicated by gradational zones with meteoric evidences (the abnormal high value of terrestrial element mainly). Prolonged subaerial exposure indicators are generally absent at the measured sections. Previous studies mostly favored the placement of sequence boundaries in the middle on the falling limbs of Fischer plots, representing the maximum rate of accommodation loss (Goldhammer et al. 1990; Chen et al. 2001). In this study, the sequence boundaries are placed in the lowermost point of the falling limbs where the terrestrial element is of most concentrated (Fig. 5, 6, 7 and 8). In many carbonate platform-interior successions, third-order depositional sequences commonly consist of two components in view of the weak development of the lowstand systems tract; thus each third-order sequence comprises an overall rising limb followed by a falling limb of accommodation change, with superimposed shorter-term fluctuations (Read and Goldhammer 1988; Goldhammer et al. 1990).

Nine third-order sequences are identified in the research area: 5 sequences in Yingshan Group and 4 in Yijianfang Group respectively. Chen and Guo (2016, internal data) identified 7 third-order sequences of Yingshan Group in Bachu area, Tarim Basin, which corresponded to 7 eustatic cycles of Floian and Dapingian. The Yingshan Group in Yuejin-Tuoputai area is buried so deep that YJ1X well is just drilled into Yingshan Group for a short depth (Northwest Petroleum Bureau of Sinopec 2016). Therefore, only Yijianfang Group and the upper member of Yingshan Group are studied in this research. Because this research is the continuation of Chen's (2016), the two-third-order sequences above and below of the interface between Yingshan and Yijianfang Group are named as Sq7 and Sq8. Then, the numbers of other sequences are also named in this order, which can make our research correspond to the previous study of Chen easily. The upper member of Yingshan Group can be divided into 5 third-order sequences (Sq3–Sq7) and their thicknesses vary a lot (17–30 m). Then, Yijianfang Group can be divided

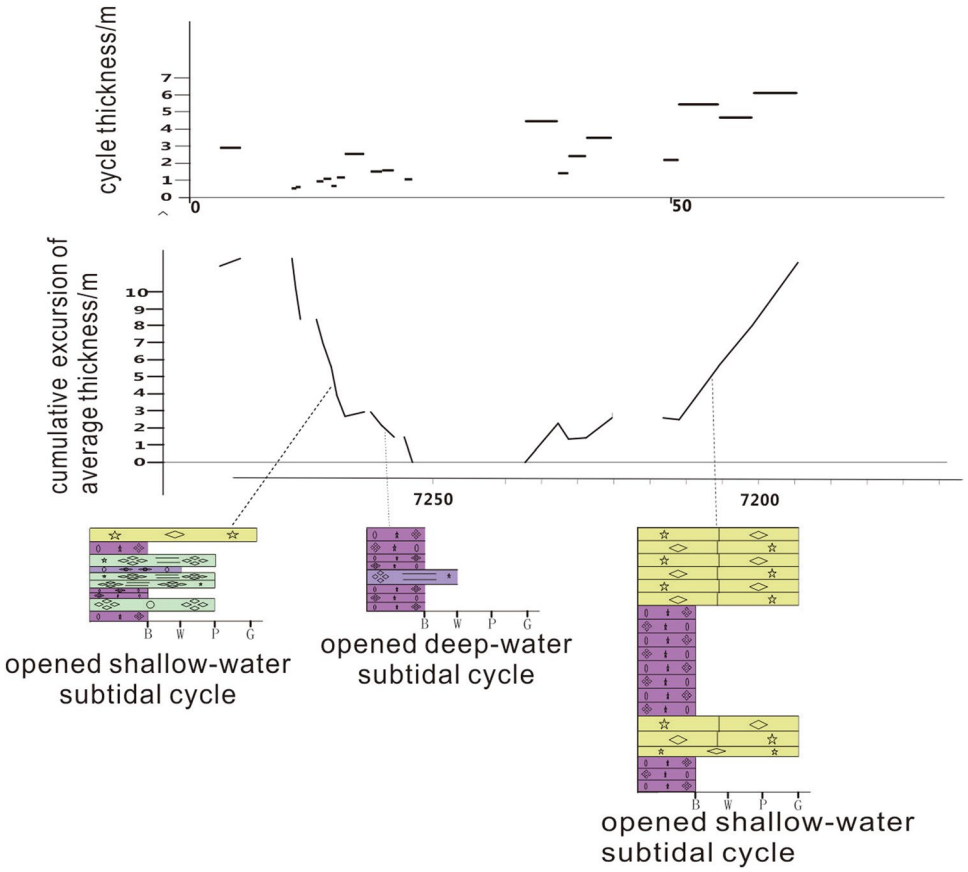

Fig. 5 Fischer diagram for the cycle superposition patterns and vertical sedimentary-faces variation of Yuejin well upper member of Yingshan Group-Yijianfang Group. The instruction for the recurrent vertical cycle superposition patterns: the open shallow-water subtidal cycle forms in the falling stage of third-order sea-level. It commonly starts from LY4 and then changes upward to LY6. The open deep-depth subtidal cycle forms in the falling stage of third-order sea-level. It commonly starts from LY2 and then changes upward to LY3. The open-marine shallow-depth subtidal cycle forms in the relatively stable or slightly-rising stage of third-order sea-level. It commonly starts from LY2 and then changes upward to LY4 and LY6. SB is the interface of sequences

into 4 third-order sequences (Sq8–Sq11) and their thicknesses also vary a lot (8 m–40 m). Due to the deep water, the sq10 and sq11 are influenced by "the loss of subtidal cycle". The sequences can be made up into sequence sets in bigger scale, upper sequence set (Sq3–Sq7)and lower sequence set (Sq8–Sq11).

Sq3–Sq7

In this study, because the sample interval is too big to identify sequences in YJ1X, we only describe these 5 sequences developed in Tuoputai area. Some features can be found that these sequences in Tuoputai area are at the rising-descending cycle of Fisher Curve. This indicates a phenomenon, accumulative in long term and maybe periodic in short term, that the accommodation space keeps steady. These sequences develop in semi-restricted shallow-middle subtidal facies.

Sq3

In Tuoputai area, the transgressive system tract (TST) is a semi-restricted shallow-water subtidal cycle. The bottom of the cycle is LT3, The upward increase of pelletoid indicates a shallowing-upward water body. Then, the high system tract (HST) is a semi-restricted shallow-water subtidal cycle. The bottom of the cycle is LT4 and the top is LT1, which represents a shallowing-upward water body and increasing-upward hydrodynamic force.

Sq4

In Tuoputai area, the transgressive system tract (TST) is a semi-restricted shallow-water subtidal cycle, the bottom of the cycle is LT4, and the upward increase of pelletoid(LT1) indicates a shallowing-upward water body. Then, the high system tract (HST) is a semi-restricted shallow-water subtidal cycle. The bottom of the cycle is unknown because the lackness of rock samples. And the top is LT1, which represents a shallowing-upward water body and increasing-upward hydrodynamic force.

Sq5, Sq6

The characteristic of sq5 is similar to that of sq4, and the difference is that there is a new cycle in HST. The bottom of the cycle is LT4 and the top of the cycle is LT3, which indicates a deeper water body. Also, the sq6 has the same features with sq4. The difference is the bottom of the cycle is LT3 in HST and changing into LT2 and LT1 upward, which

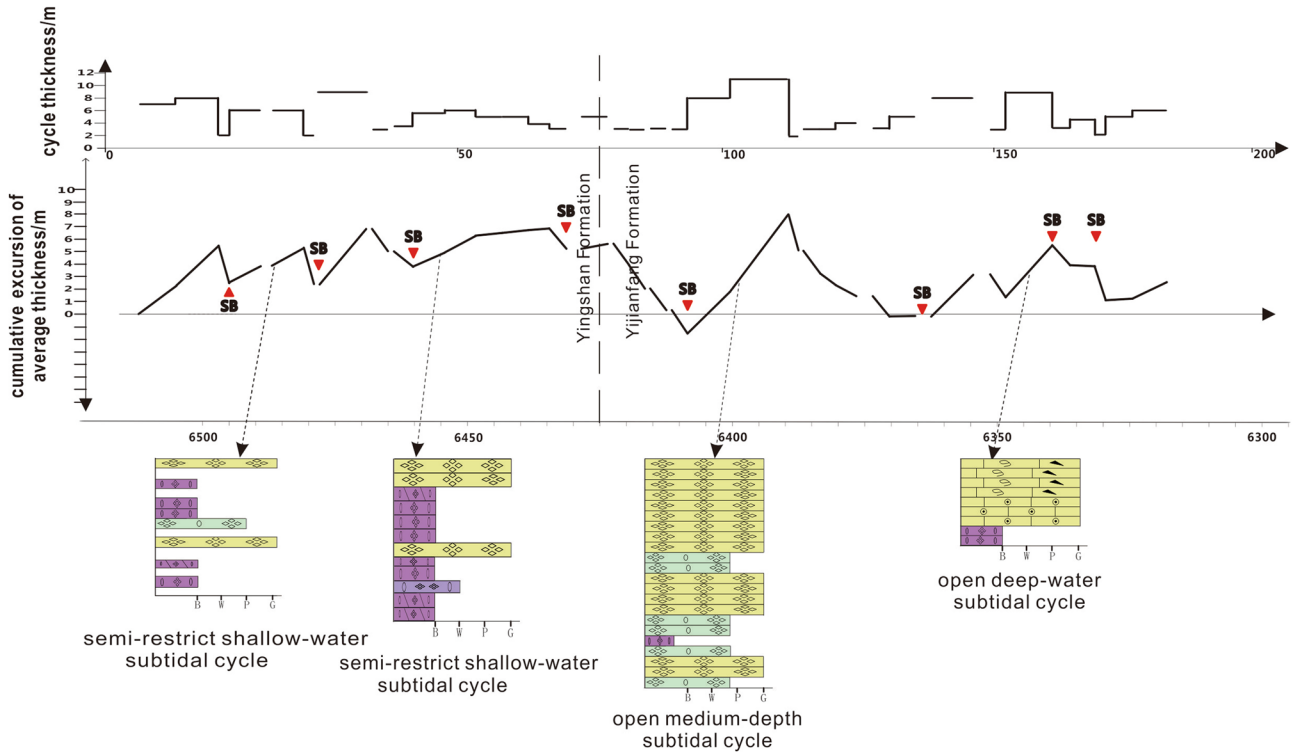

Fig. 6 Fischer diagram for the cycle superposition patterns and vertical sedimentary-faces variation of S114 well upper member of Yingshan Group. The instruction for the recurrent vertical cycle superposition patterns: the semi-restricted shallow-depth subtidal cycle forms in the rising stage of third-order sea-level. It commonly starts from LT4 and then changes upward to LT1 or LT2. The open middle-water subtidal cycle forms in the rising stage of third-order sea-level. It commonly starts from LT2 and then changes upward to LT1.The open-marine shallow-water subtidal cycle forms in the further rising stage of third-order sea-level. It commonly starts from LT5 and then changes upward to LT2 or LT6 or LT8. SB is the interface of sequences

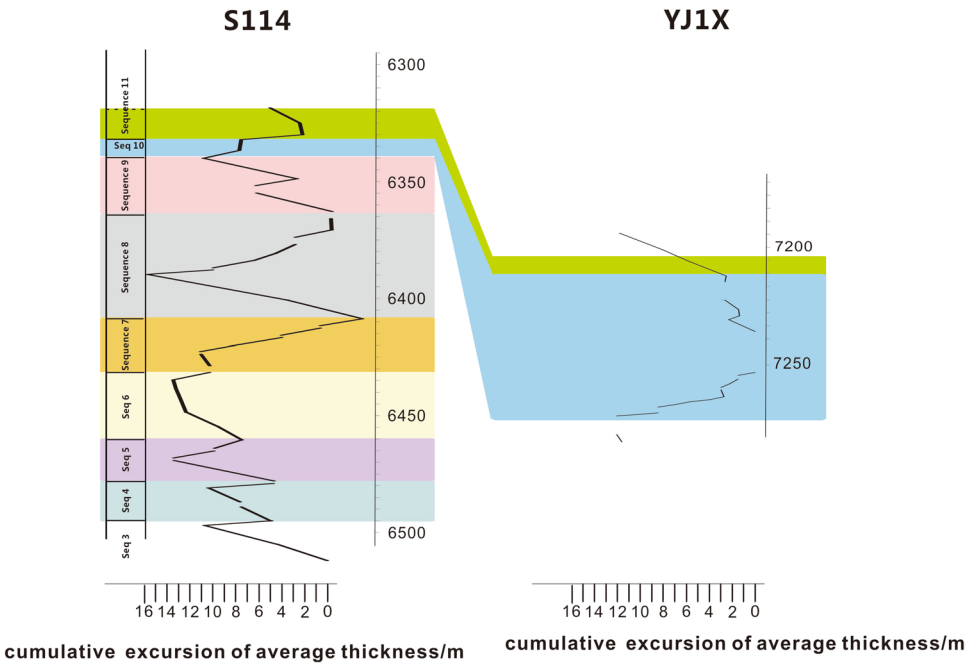

Fig. 7 Yuejin-Tuoputai well-to-well sequence correlation

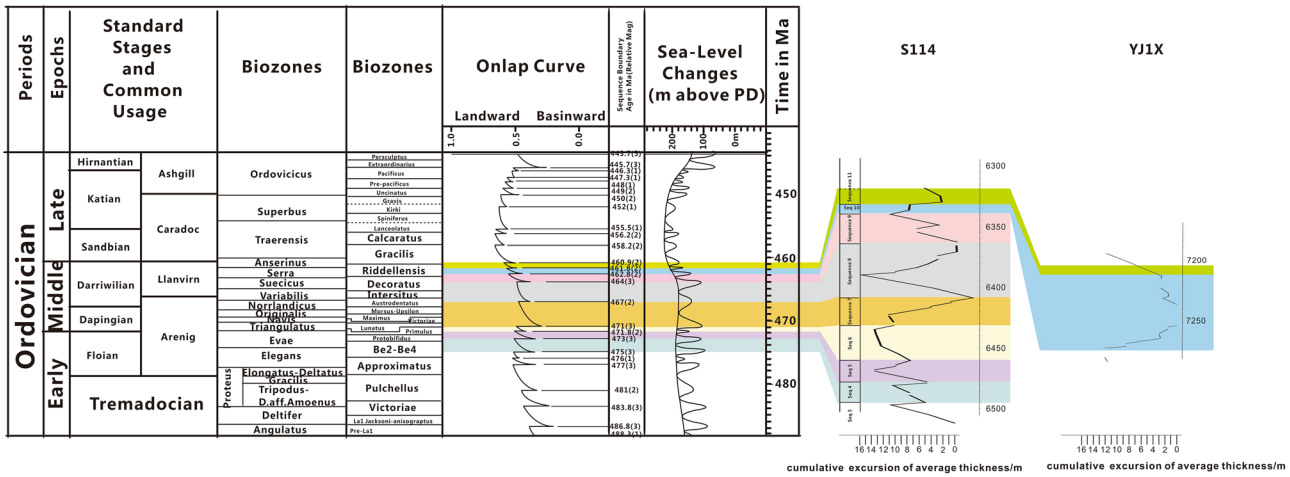

Fig. 8 The correlation between t third-order sequences (upper member of Yingshan Group to Yijianfang Group of Yuejin-Tuoputai area) and standard global sea-level fluctuation curve (accommodation space). The number of third-order sequences corresponded to the cycle number of transgression-regression and coastal onlap in short-term global sea-level change curves. This indicates third-order sequences are mainly controlled by the change of global sea-level. Floian-Darriwilian sea-level change curve based on Fischer plots show the same characteristics with global sea-level change curves of Haq and Schutter (2008). Four third-order sequences can be identified in Yingshan group, and four in Yijianfang group either

indicates water falls gradually and the relative sea level varies slightly.

Sq7

It is composed of semi-restricted shallow-depth subtidal cycle. The bottom of cycle in TST is LT2 and the top is LT1, which indicates shallow-middle subtidal environment. Three types of cycle are identified in HST, the bottom is LT4, LT3 and LT2, respectively, and the top is LT1. And three types of cycles appear in order from bottom to top, indicating the gradual shallow water. To be noted, the cycle developed in Sq7 is the most abundant in the upper Yingshan Group, indicating that the relative sea-level change is the slowest, the rate of subsidence may be the slowest at this time.

Sq8–Sq11

Some features can be found: these Fisher Curves of sequences fluctuate strongly in the middle-lower part of Yijianafang Group while keeping steady in the upper part. This indicates a phenomenon, accumulative in long term and maybe periodic in short term, that the accommodation space varies from violent to gentle. TST of sq8 and sq9 is a semi-restricted shallow-water subtidal cycle, while HST of sq9-sq11 is an open shallow-deep water subtidal cycle. Since at that time Yuejin-Tuoputai area was in the deep-water environment, all of the sequences were influenced by "the loss of subtidal cycle" and Fisher Curve showed an opposite tendency to the theoretical cure (Goldhammer et al. 1990; Osleger and Read 1991).

Sq8

It is composed mainly of semi-restricted shallow-water subtidal cycle. The TST mainly develops high-powered shallow-water cycle, the bottom is LT2 and the top is LT1. The cycle in upper HST is the continuance of Sq7, showing the continuance of deposition. Also it indicates the lackness of depositional break or subaerial exposure between Sq7 and Sq8. The cycle of HST is very complex, which is similar to Sq7 that the bottom is LT4, LT3 and LT2, respectively, and the top is LT1.

Sq9

The cycle of TST is unclear due to the lack of samples. Beginning from HST, the environment transfers from semi–restricted to open zone. It develops open shallow-water subtidal cycle. The bottom of cycle is LT9 and changes from LT6 upward to LT7 and LT8, indicating an increasing-upward hydrodynamic force. The change from ooid to clastizoic grains indicates a shallow water body and good penetration of light. And the environment is near-normal wave base. This variation of lithology represents that the water salinity changes to normal level gradually and the environment transfers from semi-restricted to open zone.

Sq10

The dramatic change of sedimentary environment started from Sq10. It completely consists of LT9. Cycle is very difficult to identify and the water condition is only based

on the content of biogenic debris. The lithology changes a lot and the type of cycle transfers to an open middle-deep subtidal one. In Yuejin area, TST is an open middle-deep water subtidal cycle, which can be divided into three types. The first cycle consists of LY4 completely. The second is composed of LY2 and LY3. The third is composed of LY2 entirely. HST develops four types of cycle. The first cycle is composed of LY2, LY5 and LY6; the second cycle has LY6 and LY2; the third one consists of LY3 and LY4; the last one is composed of LY3 and LY6. All the four cycles represent a shallowing-upward water body. The complexity and variation of cycle illustrate that the flunctuation of sea level is complicated and the environment is more complex than Tuoputai area.

Sq11

Sq11 forms in the open-platform deep-water subtidal environment on the whole and also shows the characteristics of gentle-slope environment in Tuoputai area. The cycle is composed of LT9 entirely and is the continuance of Sq10. In Yuejin area, TST of Sq11 is a shallowing-upward cycle, the bottom is LY2 and the top is LY6. Its HST is similar to Tuoputai's that consisted of LY2, reflecting the deepening of water. Compared with Tuoputai area, Yuejin area has a more obvious change in water and the sea level has an obvious drop between TST and HST.

Correlation of depositional sequences in the Lower-Middle Ordovician and controls on platform development

A large number of previous studies had been conducted on Middle-Lower Ordovician in Tarim Basin. However, there was no unique conclusion for the identification of third-order sequence, and the number of the sequences identified varied a lot. By combining the methods of sequence stratigraphy and biostratigraphy, Yu (1996) divided Yingshan Group into 4 third-order sequences. Qu (1997) divided lower Ordovician into 4 third-order sequences, using several seismic sections. Based on the outcrops of Keping area, Chen et al. (2004) divided Yingshan Group into 4 third-order sequences. Yingshan Group had been divided into 3 third-order sequences by Zhao (2009), and outcrop, drilling and seismic sequence played an important role in the research. Hu et al. (2010) divided lower Ordovician into 4 third-order sequences in Keping area in 2010. By using the variation tendency of magnetic susceptibility, Wu (2012) divided Yingshan Group into 6 third-order sequences. Changsonglin **(后面没对应的文献)** divided Yingshan Group into 4 third-order sequences, and Yijianfang Group was identified as one-third-order sequence here. Based on several comprehensive materials (e.g. sedimentary materials, well-logging data and diagenetic marking), Yijianfang Group was identified as a complete third-order sequence. In conclusion, agreement could not be found among the research results mentioned above, which might be caused by the notable variation of sedimentary faces in vertical and horizontal direction. Also, this variation could not be observed and tracked easily (Zhang et al. 2015).

In this study, nine third-order sequences were identified in the thick limestone successions of the Upper Yingshan and Yijianfang Group in the Central Tarim based on detailed borehole core investigations, vertical facies and cycle stacking patterns as revealed by Fischer plots. Within equivalent stratigraphic successions, these sequences can be correlated with those in the Chronology of Paleozoic Sea-Level Changes (Haq and Schutter 2008). This scenario suggests a major control in particular, of third-order, eustatic changes on deposition of the Lower-to Middle Ordovician carbonate sequences in the Tarim Basin, although lithofacies may vary in different areas due to regional tectonics, platform morphology, sediment supply, climate and short-term sea-level changes. In turn, this scenario further improves the previous stratigraphic classification of the Lower-to Middle Ordovician in the Tarim Basin. Previous biostratigraphic studies suggested that the Yingshan and Yijianfang Groups were roughly constrained within the Lower-Middle Ordovician (Floian, Dapingian and Darriwilian), although not exactly defined for the lower and upper boundaries. At the S114 section, however, it should be noted that this group is separated from the overlying Qiaerbake Group by the first occurrence of nodular limestones, which can be easily recognized in the field. However, the cycle stacking patterns revealed in this study provide a useful independent constraint to place the Middle-Upper Ordovician boundary in the platform successions of the Tarim Basin through matching the cycle and sequence patterns elsewhere.

The larger scale sequence stacking patterns show a longer term (second-order) increase in accommodation space from Sq3 to Sq6 and subsequent decrease in Sq7. But in Seq 8 to Seq 11, the accommodation space shows violent fluctuation. These reflected a longer term (second-order) synoptic sea-level rise-fall-rise trend on which third-order sea level fluctuations were superimposed during this period. This scenario is different from the longer-term patterns of sea-level changes elsewhere (Haq and Schutter 2008), and this is likely to have resulted from a different tectonic history from other areas.

Lateral facies variations within the sequence framework across the studied sections show that the open-marine subtidal facies, predominate at the two sections during the Darriwilian, suggesting that an open-marine intraplatform (or intrashelf) bay or depression developed at the two localities and extended eastward to link with the Manjiaer Depression. A thicker strata thickness was found in Yuejin

area, which could have resulted in a higher depositional rate there, thereby accommodating a thicker carbonate succession, about 1.5 as thick as the Tuoputai area.

Conclusions

1. Six lithofacies(LY1-LY6) can be identified in Yuejin area and nine(LT1-LT9) in Tuoputai area, which are interpreted to have been deposited in semi-restricted shallow subtidal, to open deep subtidal environments on a carbonate ramp system.
2. Two main types of meter-scale, shallowing-upward cycles are recognized: semi-restricted subtidal and open subtidal. The semi-restricted subtidal cycles, predominating over the middle-upper Yingshan Group and the lower Yijianfang Group, commence with bindstone and are capped by pelletoid grainstone and bindstone with peloidal grains. In contrast, the open middle-deep water subtidal cycles, dominating the upper Yijianfang Group, are dominated by clastizoic grainstone and clastizoic bindstone.
3. Nine third-order depositional sequences (Sq3–Sq11) are distinguished and are generally composed of two parts: the lower thicker semi-restricted shallow-middle water subtidal facies and the upper thinner open middle-deep water subtidal facies.
4. A third-order eustatic control on the deposition of these sequences because these sequences can be correlated with those in the Global standard Sea-Level Changes within equivalent stratigraphic successions. The high-frequency, meter-scale, and shallowing-upward cycles were likely formed in response to high-frequency eustatic sea-level fluctuations which were superimposed on third-order sealevel changes. The larger scale sequence sets indicate that these sequences were also controlled by longer term sea-level changes likely induced by the tectonic evolution of the Tarim Basin. Differential tectonic subsidence on the carbonate platform further controlled the spatial distribution of the various facies and depositional rate.

References

Adamxs RD, Grotzinger JP (1996) Lateral continuity of facies and parasequences in Middle Cambrian platform carbonates, Carrara Group, southeastern California. USA. J Sediment Res. 66:1079–1090

Badena B, Aurell M (2010) Facies models of a shallow-water carbonate ramp based on distribution of non-skeletal grains (Kimmeridgian, Spain). Facies 56:89–110

Badenas B, Aurell M, Grocke DR (2005) Facies analysis and correlation of high-order sequences in middle-outer ramp successions: variations in exported carbonate on basin-wide $\delta 13C_{carb}$ (Kimmeridgian, NE Spain). Sedimentology 52:1253–1275

Balog A, Haas J, Read JF, Coruh C (1997) Shallow marine record of orbitally forced cyclicity in a Late Triassic carbonate platform, Hungary. J Sediment Res 67:661–675

Bayet-Goll A, Geyer G, Wilmsen M, Mahboubi A, Moussavi-Harami R (2014) Facies architecture, depositional environments, and sequence stratigraphy of the Middle Cambrian Fasham and Deh-Sufiyan Groups in the central Alborz. Iran. Facies. 60:815–841

Bosence DWJ, Wood JL, Rose EPF, Qing H (2000) Low-and high frequency sea-level changes control peritidal carbonate cycles, facies and dolomitization in the Rock of Gibraltar (Early Jurassic, Iberian Peninsula). J Geol Soc. 157:61–74

Bosence D, Procter E, Aurell M, Kahla AB, Boudagher-Fadel M, Casaglia F, Cirilli S, Mehdie M, Nieto L, Rey J (2009) A dominant tectonic signal in high-frequency, peritidal carbonate cycles? A regional analysis of Liassic platforms from western Tethys. J Sediment Res 79:389–415

Chen DZ, Tucker ME (2003) The Frasnian-Famennian mass extinction: insights from high-resolution sequence stratigraphy and cyclostratigraphy in South China. Palaeogeogr Palaeoclimatol Palaeoecol 193:87–111

Chen DZ, Tucker ME, Jiang MS, Zhu JQ (2001) Long–distance correlation between tectonic–controlled, isolated carbonate platforms by cyclostratigraphy and sequence stratigraphy in the Devonian of South China. Sedimentology 48:57–78

Chen DZ, Qing HR, Yang C (2004) Multistage hydrothermal dolomites in the Middle Devonian (Givetian) carbonates from the Guilin area, South China. Sedimentology 51:1029–1051

Chen DZ, Guo ZH, Jiang MS, Guo C, Ding Y (2016) Dynamics of cyclic carbonate deposition and biotic recovery on platforms during the Famennian of Late Devonian in Guangxi, South China: constraints from high-resolution cycle and sequence stratigraphy. Palaeogeogr Palaeoclimatol Palaeoecol 448:245–265

DUNHAM, R.J., 1962. Classification of carbonate rocks according to depositional texture. In: Ham WE (ed) Classification of carbonate rocks. AAPG Mem., 1, 108–121

Elrick M (1995) Cyclostratigraphy of middle devonian carbonates of the eastern Great Basin. J Sediment Res 65:61–79

Elrick M, Read JF (1991) Cyclic ramp-to-basin carbonate deposits, Lower Mississippian, Wyoming and Montana; a combined field and computer modeling study. J Sediment Petrol 61:1194–1224

FISCHER, A. G., 1964. The lofer cyclotems of the alpine Triassic. In: Merriam DF (ed) Symposium on Cyclic Sedimentation. Kansas State Geol Surv Bull 169, 107–149

Fischer AG, Bottjer DJ (1991) Orbital forcing and sedimentary sequences. J Sediment Petrol 61:1063–1069

Goldhammer RK, Dunn PA, Hardie LA (1987) High-frequency glacio-eustatic sea-level oscillations with Milankovitch characteristics recorded in Middle Triassic platform carbonates in northern Italy. Am J Sci 287:853–892

Goldhammer RK, Dunn PA, Hardie LA (1990) Depositional cycles, composite sea-level changes, cycle stacking patterns, and the hierachy of stratigraphic forcing: examples from Alpine Triassic platform carbonates. Geol Soc Am Bull 102:535–562

Goldhammer RK, Lehmann PJ, Dunn PA (1993) The origin of high frequency platform carbonate cycles and third-order sequences (Lower Ordovician El Paso Gp, West Texas): constraints from outcrop data and stratigraphic modeling. J Sediment Res 63:318–359

Guo F, Lai SH, Guo L (2010) Ordovician Sequence Stratigraphy and Sedimentology in the Dabantage Area, Tarim Basin. J Stratigr 34(2):135–144 **(in Chinese)**

Hamon Y, Merzeraud G (2008) Facies architecture and cyclicity in a mosaic carbonate platform: effects of fault-block tectonics (Lower Lias, Causses platform, south-east France). Sedimentology 55:155–178

Han L, Gao B, Xu D et al (2015) The characteristic of Pb isotopic compositions in different chemical fractions in sediments from Three Gorges Reservoir, China. Environ Pollut 206:627–635

Haq BU, Schutter SR (2008) A chronology of Paleozoic sea-level changes. Science 322:64–68

HE, D.F., LI, D. S., 1996. The structure evolution and accumulation of oil and gas in tarim basin [M]. Geological publishing house

Heasley EC, Worden RH, Hendry JP (2000) Cement distribution in a carbonate reservoir: recognition of a palaeo oil-water contact and its relationship to reservoie quality in the Humbly Grove field, onshore, UK. Mar Pet Geol 17:639–654

Hendry JP (2002) Geochemical trends and palaeohydrologcial significance of shallow burial calcite and ankerite cements in Middle Jurrassic strata on the East Millands Shelf (onshore UK). Sed Geol 151:149–176

Hofmann MH, Keller M (2006) Sequence stratigraphy and carbonate platform organization of the Devonian Santa Lucia Group, Cantabrian Mountains. NW-Spain. Facies 52:149–167

Hofmann A, Dirks PHGM, Jelsma HA (2004) Shallowing–upward carbonate cycles in the Belingwe Greenstone Belt, Zimbabwe: a record of Archean sea-level oscillations. J Sediment Res 74:64–81

Hu MY, Qian Y, Hu ZG (2010) Carbon isotopic and element geochemical responses of carbonate rocks and Ordovician sequence stratigraphy in Keping area, Tarim Basin. Acta Petrol Mineral 29(2):199–205 **(in Chinese)**

Husinec A, Basch D, Rose B, Read JF (2008) FISCHERPLOTS: an Excel spreadsheet for computing Fischer plots of accommodation change in cyclic carbonate successions in both the time and depth domains. Comput Geosci 34:269–277

Jia CZ, Zhao JZ (1997) The characteristics of oil and gas resources and strategic thinking of exploration and development in Tarim basin[C]. "Reasonable utilization and sustainable development of northwest water, soil and ore resource" academic symposium

Laya JC, Tucker ME, Perez-Huerta A (2013) Meter-scale cyclicity in Permian ramp carbonates of equatorial Pangea (Venezuelan Andes): implications for sedimentation under tropical Pangea conditions. Sed Geol 292:15–35

Lee MK (1997) Predicting diagenetic effects of groundwater in sedimentary basins: a modeling approach with examples. In: Montanez IP, Gregg JM, Shelton KL (Eds.), Basin-wide diagenetic patterns: Integrated petrologic, geochemical and hydrologic considerations. 180 SEPM Spec. 57:3–14

Li YT, Ye N, Yuan XY, Huang QY, Su BR, Zhou RQ (2015) The geological and geochemical characteristics of silicified hydrothermal fluid in Shunnan 4 Well in the tarim basin [J]. Petrol Gas Geol 2015(06):934–944

Lu X, Wang Y, Tian F, et al. New insights into the carbonate karstic fault system and reservoir formation in the Southern Tahe area of the Tarim Basin[J]. Marine & Petroleum Geology, 2017, 86

Montaenz IP, Osleger DA (1993) Parasequece stacking patterns, third-order accommodation events, and sequence stratigraphy of Middle to Upper Cambrian platform carbonates, Bonanza King Group, southern Great Basin. In: Loucks B, Sarg JF (eds) Recent advances and applications of carbonate sequence stratigraphy, vol 57. AAPG Memoir., pp 305–326

Montanez IP (1997) Secondary porosity and late diagenetic cements of the Upper Knox Group, central Tennesse region: a temporal and spatial history of fluid flow conduit development within the Knox regional aquifer, In: Montanez IP, Gregg JM, Shelton KL (Eds.), Basin-wide diagenetic patterns: Integrated petrologic, geochemical and hydrologic considerations. SEPM Spec. Pub., 57: 101-117

Mutti M, Simo J (1993) Stratigraphic patterns and cycle-related diagenesis of upper Yates Group, Permian, Guadalupe mountains. In: Loucks B, Sarg JF (eds) Recent advances and applications of carbonate sequence stratigraphy, vol 57. AAPG Memoir, pp 515–534

Osleger DA, Read JF (1991) Relation of eustasy to stacking patterns of meter-scale carbonate cycles, late Cambrian, USA. J Sediment Res 61:1225–1252

Osleger DA, Read JF (1993) Comparative analysis of methods used to define eustatic variations in outcrop: late Cambrian interbasinal sequence development. Am J Sci 293:157–216

Qu H, Xu HD, Guo QJ (1997) Study on sequence stratigraphy of Ordovician in North Tarim Basin. China Univ Geosci 11(1):8–13 **(in Chinese)**

Read JF, Goldhammer RK (1988) Use of Fischer plots to define third-order sea-level curves in Ordovician peritidal cyclic carbonates. AppL Geol 16:895–899

Sadler PM, Osleger DA, Montanez IP (1993) On the labeling, length, and objective basis of Fischer plots. J Sediment Res 63:360–368

Schlager W (2005) Carbonate Sedimentology and Sequence stratigraphy. SEPM Concepts in Sedimentology and Paleontology, 8, Tulsa, Oklahoma, USA

Strasser A, Hillgartner H (1998) High-frequecy sea-level fluctuations recorded on a shallow carbonate platform (Berriasian and Lower Valanginian of Mount Salève, French Jura). Ecl Geol Helv 91:375–390

Strasser A, Hillgartner H, Hug W, Pittet B (2000) Third-order depositional sequences reflecting Milankovitch cyclicity. Terra Nova 12:303–311

Tian F, Jin Q, Lu X et al (2016) Multi-layered ordovician paleokarst reservoir detection and spatial delineation: a case study in the Tahe Oilfield, Tarim Basin, Western China[J]. Mar Pet Geol 69:53–73

Tian F, Lu X, Zheng S et al (2017) Structure and filling characteristics of paleokarst reservoirs in the northern tarim basin, revealed by outcrop, core and borehole images[J]. Open Geosci 9:1

Tucker ME, Garland J (2010) High-frequency cycles and their sequence stratigraphic context: orbital forcing and tectonic controls on Devonian cyclicity, Belgium (The André Dumont medallist lecture). Geol Belgica 13:213–240

Vail PR, Audemard F, Bowman S, Eisner P, Perez C (1991) The stratigraphic signatures of tectonics, eustasy and sedimentology—an overview. In: Einsele G, Ricken W, Seilacher A (eds) Cycles and events in stratigraphy. Springer, Berlins, pp 617–659

Van Wagoner JC (1995) Sequence stratigraphy: an integrated technique for exploration and exploitation, part I: Concepts and well log, core, and outcrop examples. Seg Techn Program Expanded Abs 14(1):1521

Vincent SJ , Morton AC , Carter A et al (2007) Oligocene uplift of the Western Greater Caucasus: an effect of initial Arabia-Eurasia collision. Terra Nova 19(2):160–166

Vossler SM, Pemberton G (1988) Skolithos in the Upper Cretaceous Cardium Group; an ichnofossil example of opportunistic ecology. Lethaia 21:351–362

Wang EH (2013) Tarim basin middle-upper ordovician carbonate strata sequence framework and its control of reef beach body. Sci Technol Rev 31(10):24–29 **(in Chinese)**

Wang ZM, Jiang RQ, Wu JC (2011) Sequence stratigraphic characteristics of Cambrian Ordovician carbonate rocks in Tarim Basin. Petrol Geol 2:1672–7703 **(in Chinese)**

Wu ZJ, Yao JX, Chen LQ (2012) Ordovician sequence stratigraphy of Keping area, northwest Tarim Basin. Acta Petrol Mineral 31(6):875–884 **(in Chinese)**

Xu GQ, Wu WH et al (2006) The seismic identification and development distribution of the reef beach in the upper Ordovician in Tarim basin and Tianhe area[J]. Mineral Rocks 26(2):80–86

Yu BS (1996) Sequence stratigraphic framework of the Cambrian-Ordovician in Northern Tarim Basin. Acta Mineral Sinica 16(3):298–303 **(in Chinese)**

Zhang YQ, Chen DZ, Zhou X, Guo ZH, Wei W, Mutti M (2015) Depositional facies and stratal cyclicity of dolomites in the Lower Qiulitag Group (Upper Cambrian) in northwestern Tarim Basin, NW China. Facies 61:1–24

Zhao ZJ, Pan WQ, Zhang LJ (2009) Sequence stratigraphy in the Ordovician in the Tarim Basin. Geotecton Metallog 33(1):175–188 **(in Chinese)**

Zheng HR, Wu MB, Wu XW, Zhang T, Liu CY (2007) Oil-gas exploration prospect of dolomite reservoir in the Lower Paleozoic of Tarim Basin. Acta Petrolei Sin. 28:1–8 **(in Chinese)**